Observation of magnetic edge state in graphene nanoribbons

V. L. Joseph Joly, Manabu Kiguchi, Si-Jia Hao, Kazuyuki Takai, and Toshiaki Enoki
Department of Chemistry, Tokyo Institute of Technology, 2-12-1 Ookayama, Meguro-ku, Tokyo 152-8551, Japan

Ryohei Sumii and Kenta Amemiya
Institute of Materials Structure Science, High Energy Accelerator Research Organization, Tsukuba, Ibaraki 305-0801, Japan

Hiroyuki Muramatsu, Takuya Hayashi, Yoong Ahm Kim, and Morinobu Endo
Faculty of Engineering and Institute of Carbon Science and Technology, Shinshu University, 4-17-1 Wakasato, Nagano shi, 380-8553, Japan

Jessica Campos-Delgado and Florentino López-Urías
Advanced Materials Department, IPICYT, Camino a la Presa San José 2055, Col. Lomas 4a. sección, San Luis Potosí 78216, Mexico

Andrés Botello-Méndez and Humberto Terrones
Institute of Condensed Matter and Nanosciences (IMCN), Université Catholique de Louvain, Place Croix du Sud 1, B-1348 Louvain-la-Neuve, Belgium

Mauricio Terrones
Department of Materials Science and Engineering and Chemical Engineering, Polytechnic School, Carlos III University of Madrid, Avenida Universidad 30, Leganés, 28911 Madrid, Spain

Mildred S. Dresselhaus
Department of Physics and Department of Electrical Engineering and Computer Science, Massachusetts Institute of Technology, 77 Massachusetts Avenue, Cambridge, Massachusetts 02139-4307, USA

(Received 19 March 2010; revised manuscript received 25 May 2010; published 22 June 2010)

The electronic structure and spin magnetism for few-layer-graphene nanoribbons synthesized by chemical vapor deposition have been investigated using near-edge x-ray absorption fine structure (NEXAFS) and electron-spin resonance (ESR). For the pristine sample, a prepeak was observed below the π^* peak close to the Fermi level in NEXAFS, indicating the presence of additional electronic states close to the Fermi level. The intensity of this prepeak decreased with increasing annealing temperature and disappeared after annealing above 1500 °C. The ESR spectra, which proved the presence of localized spins, tracked the annealing-temperature-dependent behavior of the prepeak with fidelity. The NEXAFS and ESR results jointly confirm the existence of a magnetic edge state that originates from open nanographene edges. The disappearance of the edge state after annealing at higher temperatures is explained by the decrease in the population of open edges owing to loop formation of adjacent graphene edges.

DOI: 10.1103/PhysRevB.81.245428 PACS number(s): 73.22.Pr, 75.75.−c, 76.30.−v

I. INTRODUCTION

Graphene, the most recent addition to the family of carbon nanostructures has received unprecedented attention due to its two-dimensional crystal structure and unique electronic structure.[1] The features of the Dirac-massless fermion with a linear dispersion of π bands at the Fermi level in single-layer graphene give rise to a variety of exotic electronic properties, even at room temperature.[2,3] When the size of a graphene sheet is reduced to a few nanometer, other interesting phenomena could be expected due to the growing contribution of the edges to the electronic structure. Here, an edge of nanographene with whatsoever shape can be expressed simply as a combination of zigzag and armchair edges. Interestingly, the band structure of nanographene at the Fermi level can be distinguished with respect to its edge geometry. Indeed, theoretical and experimental studies showed the presence of a localized nonbonding π state (edge state) in the zigzag-shaped edge regions, whereas the armchair edge does not exhibit this feature.[4–12] More importantly, the localized edge-state electrons are strongly spin polarized[13] and coupled with the itinerant π carriers. Therefore, nanographene can exhibit an interesting interplay between magnetism and electron transport similar to traditional *s-d* metal magnets.[10] In addition, the electronic properties, particularly electron transport in nanographene strongly depend on its shape. Accordingly, the unconventional electronic and magnetic features of nanographene not only raise new fundamental issues in condensed-matter physics but also can be a promising target for potential applications in electronics/spintronics.[10–12]

Here, in investigating the unconventional electronic and magnetic properties of nanographene and employing these properties in device applications, it is particularly important to confirm the presence of edge states and their geometrical variations. Recently, experimental efforts have been made for such a confirmation using several techniques such as scanning tunneling microscopy (STM)/scanning tunneling

spectroscopy (STS), near-edge x-ray absorption fine structure (NEXAFS), electron-spin resonance (ESR), etc. Indeed, STM/STS observations on carefully prepared graphene edges[6–9] have demonstrated both the existence of a finite density of states assigned to the edge state at the Fermi level along the zigzag edge, and the extreme sensitivity of the edge state to the modifications of the edge geometry and chemical environment. In the NEXAFS experiments on the carbon *K* edge, the observation of an edge state around the Fermi level has been claimed in a nanographite sample that was grown on a clean Pt(111) surface.[14] However, a possible contribution from metal-induced gap states,[15] at the Fermi level of nanographene owing to state mixing between graphene π electrons and metal *d* bands, could obscure the detection of an edge state in this experiment. From the magnetism approach, the ESR technique can offer a sensitive tool for detecting the localized spins of the edge state, as previous reports have unambiguously demonstrated the spin degree of freedom of the edge state in nanographene.[16–19]

However, it should be noted that all these experimental techniques measure either the electronic or the magnetic state only, and therefore they are insufficient to prove the presence of an edge state that is magnetic. In other words, it is particularly important to demonstrate that the edge state present in the nanographene edge is magnetic by testing a sample with a combination of electronic and magnetic techniques. In the present work, by combining NEXAFS and ESR experiments, we conclusively show the presence of a magnetic edge state in a graphene nanoribbon (NR) sample synthesized by Campos-Delgado *et al.*[20] This highly crystalline sample is composed of few-layer-graphene (2–40 layers) nanoribbons of length 20–30 μm and width 20–300 nm. The structural characterization of the pristine sample revealed the presence of a large population of open edges and that makes it a suitable system to investigate the presence of edge states. More interestingly, the pristine sample when annealed at higher temperatures in an Ar atmosphere, exhibited a unique structural change, viz., the loop formation by coalescing the open edges in the adjacent nanographene layers.[21] The loop formation starts to occur at an annealing temperature of 1500 °C and becomes significant at higher temperatures. Since the edge state exists at the open edges, there must be a corresponding decrease in the edge-state density with increasing loop formation. In other words, the loop formation gives us the opportunity to control the relative ratio of the edge carbon atoms to the interior carbon atoms by varying the annealing temperature, which can, in turn, help to probe the variation in the density of edge states. We have, thus, investigated these graphene nanoribbons, which have been annealed at different temperatures, by NEXAFS and ESR techniques.

II. EXPERIMENTAL

The chemical vapor deposition (CVD) grown graphene nanoribbon samples were synthesized by the pyrolysis of an aerosol precursor composed of ferrocene, thiophene, and ethanol.[20] The pristine sample (NR) was annealed at 1000 °C, 1500 °C, and 2000 °C in an Ar atmosphere for 30 min for each sample to get NR1000, NR1500, and NR2000, respectively. The carbon *K*-edge NEXAFS was measured at the soft x-ray beam line BL-7A in the Photon Factory in the Institute of Materials Structure Science, Tsukuba, Japan.[22] A powder sample was mounted on a Ta plate and loaded into the NEXAFS measurement chamber maintained in ultrahigh vacuum (10^{-9} Torr). NEXAFS spectra were then obtained by measuring the sample photocurrent (total electron yield method). The photon energy was calibrated with respect to the C 1*s* to π^* peak position of highly oriented pyrolytic graphite (HOPG) at 285.5 eV. ESR measurements were performed in the X-band region with a sample in vacuum in the range temperatures of 4–300 K.

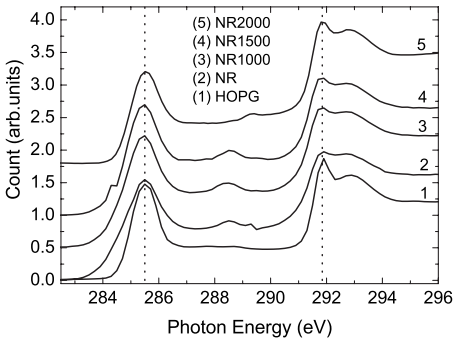

FIG. 1. Carbon *K*-edge NEXAFS spectra of the pristine graphene NR, NR1000, NR1500, and NR2000. The pristine sample (NR) and HOPG are also given for comparison. The count value for HOPG given in the figure is reduced to half of the original count to make it comparable with the other traces. The C 1*s* to π^*(285.5 eV) and σ^*(291.85 eV) transitions are indicated by dotted vertical lines.

III. RESULTS AND DISCUSSION

Figure 1 shows the carbon *K*-edge NEXAFS spectra of the pristine graphene NR, NR1000, NR1500, and NR2000. The NEXAFS spectra were normalized by the edge jump at 340 eV (not shown here), where the intensity is proportional to the amount of carbon. All of the nanoribbon samples show a dominant peak at 285.5 eV, which is close to the C 1*s* to π^* transition of HOPG, indicating the underlying graphitic structure of the sample. In addition to that, the peak at 291.85 eV, which is characteristic of the C 1*s* to σ^* transition, is also found for all the samples. The additional small features in between the π^* and σ^* peaks can be attributed to the C-OH, C-OOH, and C-H groups including foreign chemical species attached to the graphene edges, as observed in the oxidized graphites.[23,24] Moreover, the structure of the π^* peak did not depend on the appearance of these additional features. In the present study, we pay attention to the region just above the Fermi level of HOPG (284.36 eV),[25] in which we can expect the edge state to contribute to the NEXAFS spectra.

The broadened feature or the presence of a shoulder appearing on the low-energy side of the π^*-state peak in NR, NR1000, and NR1500 is suggestive of the presence of an additional peak around the Fermi level. This is evident in the

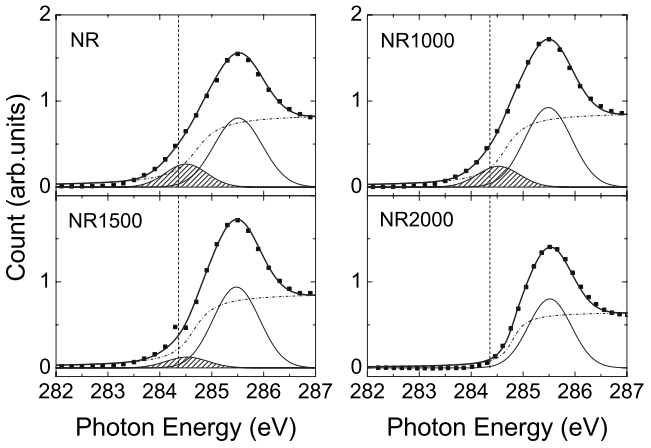

FIG. 2. The closeup of the C 1*s* to π^* peak under different annealing conditions. The data points are indicated in squares and the convoluted curve fit is given by the thick line. The deconvolution comprises two Gaussian peaks corresponding to the edge state (shaded) and the π^* state (unshaded), and a step function (dashed-dotted curve). The vertical dashed lines indicate the Fermi level of HOPG (284.36 eV) (Ref. 25).

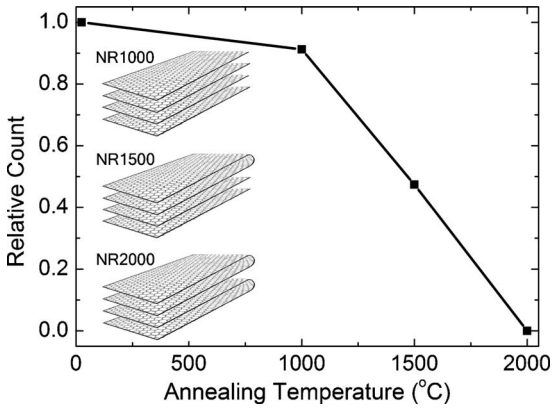

FIG. 3. The integrated NEXAFS intensity of the edge-state peak normalized to that of the pristine sample. The schematic model of the loop formation on annealing is given in the insets.

closeup view of the NEXAFS-edge region with deconvolution into two peaks and a step function as given in Fig. 2. It is clear from the curve fitting that NR2000 does not have any peak except the π^*-state peak, similar to HOPG. The extra peak appearing as the low-energy shoulder of the π^* peak can have only two possible origins, viz., dangling bonds and/or an edge state. The contribution of dangling bonds that are easily saturated by oxygen is negligibly small. Since the samples were handled under ambient conditions (before measurement), the dangling bonds, if they existed, must have been reacted to form oxygen-/hydrogen-including functional groups. The extra peaks in between π^* and σ^* in Fig. 1, belonging to the C-H, C-OH, and COOH species indicate the absence of dangling bonds. Therefore, we conclude that the low-energy shoulder of the π^* peak is due to the edge state, which can survive even in the presence of such functional groups strongly bonded to the edges.[26]

The integrated intensity of the edge-state peak obtained from deconvolution and normalized to the pristine sample is given as a function of heat-treatment temperature in Fig. 3. The intensity of the edge-state peak decreases upon elevation of the heat-treatment temperature. The intensity is reduced only slightly up to 1000 °C (NR1000) but decreases drastically on going to 1500 °C (NR1500) and finally the edge-state peak disappears above 2000 °C (NR2000). More strikingly, the position of the edge state is ~1 eV lower at 284.5 ± 0.1 eV from the π^* peak of HOPG and it is just above the Fermi level. Since the unoccupied states are observed in NEXAFS experiments, the experimental finding proves the presence of a partially filled edge state at the Fermi level, and it is in good agreement with theoretical prediction and experimental results.[4,6] It should be noted that a slight shift in the Fermi level is possible due to the charge transfer from the edge state to oxygen-including functional groups bonded to the edge carbon atoms.[27]

In order to understand the variation in the edge-state intensity with annealing temperature, the associated changes in the structure of the nanoribbon samples must be considered, as mentioned in the introduction. In the pristine sample, there is a large population of open edges. On annealing the sample at higher temperatures in an Ar atmosphere, there is a loop formation that occurs by joining the adjacent open edges of nanographenes, as shown in the inset of Fig. 3. The loop formation was found to begin at an annealing temperature of ~1500 °C, and this process consumes most of the open edges by increasing the annealing temperature to 2000 °C.[21] Since the loop formation leads to a decrease in the population of open graphene edges, a decrease in the intensity of the edge-state peak is expected. Indeed, in accordance with this structural change, the intensity of the edge-state contribution decreases sharply for the NR1500 sample (see Fig. 3) from that of the NR1000. Further elevation in the annealing temperature (NR2000) makes the edge state disappear almost completely as most of the open graphene edges combine to form loops.

Another point to be clarified here is that the feature below the π^* peak is not due to the splitting of the π^* band, as reported by Pacilé *et al.*[28] They reported an incipient peak (at 283.7 eV) just below the π^* peak for graphene, which was attributed to the splitting of the π^* band. The peak observed in the present study does not originate from the splitting of the π^* band as discussed below. Our sample showed a well-formed graphitic structure throughout the annealing temperature range,[21] and therefore, a constant intensity would be expected for the feature from the splitting of the π^* band rather than the observed systematic decrease in the intensity on annealing.

Here, we briefly comment on the temperature (1500 °C) at which the loop formation takes place. In fact, 1500 °C is a relatively inadequate temperature for the thermally activated graphitization process, which usually occurs above 2000 °C.[29] Nevertheless, a careful characterization of the heat-treated material has demonstrated that this temperature is enough to activate the formation of single loops at the edges of adjacent graphene sheets, thus having a combination of open and looped edges in the sample. Recent work of Liu *et al.*[30] on heat-treated pyrolytic graphite powders demonstrated that a temperature of 2000 °C induces the formation of double and triple loops, in good agreement with re-

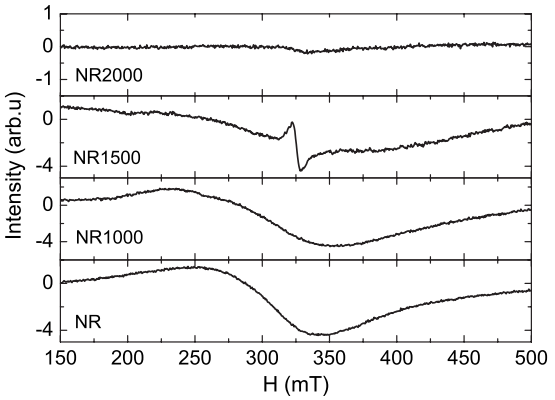

FIG. 4. Room-temperature ESR spectra of the pristine graphene NR, NR1000, NR1500, and NR2000 measured in vacuum.

sults reported by Campos-Delgado *et al.*[21] More importantly it is suggested that zigzag edges, which are chemically active due to the presence of nonbonding edge state, are easily subjected to loop formation even at temperatures lower than that of graphitization.[31]

Let us now discuss the edge state from the magnetism aspect. The room-temperature ESR spectra of the graphene nanoribbon samples are given in Fig. 4. The NR and NR1000 samples show a broad peak (peak-to-peak width, $\Delta H_{PP} \sim 100$ mT) whereas NR1500 shows a narrow Lorentzian peak with $\Delta H_{PP}=6.5-8.0$ mT and $g=2.005\pm0.001$, which is superimposed on the weak background of the broad peak. With a further increase in the annealing temperature, NR2000 does not show any significant peak except for a trace of the narrow peak. The narrow peak observed in NR1500 and NR2000 close to the free-electron g value is characteristic of the localized spins of the edge state as evident from ESR results on similar graphene-based materials having a small spin-orbit interaction.[16–19] Interestingly, the intensities of the ESR narrow peak and of the NEXAFS peak of the edge state follow the same trend in their annealing temperature dependence (see the cases of NR1500 and NR2000 in Fig. 4), confirming their common origin. The correlation between NEXAFS and ESR clearly proves the magnetic nature of the electronic state that was observed as an edge state near the Fermi level in the NEXAFS experiment.

The temperature dependence in the ESR signal assigned to the edge-state spin gives information on how the edge-state spins are incorporated into the electronic structure of graphene. Figure 5(a) shows the temperature dependence of the linewidth for NR1500 sample. The linewidth decreases linearly with the temperature upon the lowering of the temperature, and it becomes 2 mT at 4 K. This behavior is similar to that observed in activated carbon fibers,[19] which consist of a three-dimensional-disordered network of nanographene sheets. The periphery of an arbitrary-shaped graphene sheet consists of a combination of zigzag and armchair edges, the former of which has localized spin of edge-state origin. According to theoretical study,[13] the edge-state spins localized around zigzag-edge region are interacting with each other through strong intrazigzag edge ferromagnetic exchange interaction J_0 and intermediate strength in-

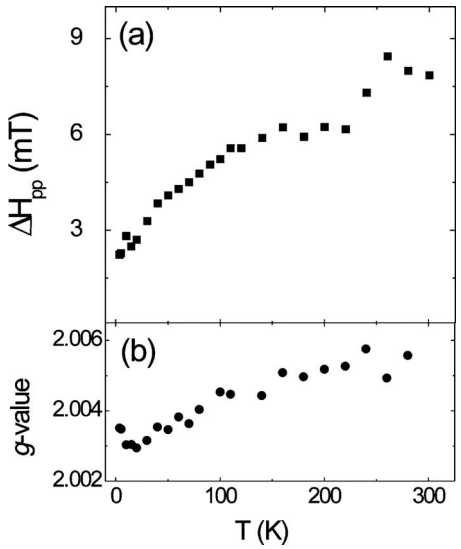

FIG. 5. Temperature dependence of (a) the linewidth and (b) the g value in the narrow ESR signal assigned to the edge-state spins for the NR1500 sample.

terzigzag edge ferromagnetic/antiferromagnetic interaction J_1 with the strengths of $J_0 \sim 10^3$ K and $J_1 \sim 10-10^2$ K, respectively. Here, it should be noted that the exchange interactions are mediated by the conduction π carriers. This means the presence of a strong coupling between the conduction π carriers and the edge-state spins. Indeed, the linear temperature dependence of the linewidth observed in the present experiments is an important indication of the presence of strong coupling between these two constituents. According to the Korringa relation,[19,32,33] the linewidth in the strongly coupled system of conduction carriers and localized spins is given as $\Delta=1/T_1 \propto T$ (T_1: spin-lattice-relaxation time), which is confirmed in the present observations. The clue on the coupling of the two spin systems is also found in the temperature-dependent g value. Figure 5(b) shows the temperature dependence of the g value. The g value decreases linearly with the temperature upon the lowering of the temperature and it reaches 2.003 at 4 K. Taking into account the Lorentzian line shape, the temperature-dependent g value is suggestive of the coexistence of two kinds of spin species having different g values, which are coupled through the exchange interaction. Indeed, the g value of the two spin systems is expressed in terms of a combination of the two g values: $g=(g_n\chi_n+g_c\chi_c)/(\chi_n+\chi_c)$, where g_n/g_c and χ_n/χ_c are the g value and the susceptibility of the edge-state spins/conduction carriers, respectively. The susceptibility of the edge-state spins shows a divergent behavior of the Curie type as the temperature approaches to zero whereas that of the conduction carriers having a Pauli paramagnetic feature is independent of the temperature. Eventually, the low-temperature limit of the g value represents the g value of the edge-state spins. In conclusion, the present experimental findings of the linear temperature dependence of the linewidth and the g value prove that the edge-state spins created around the edges of graphene nanoribbons contribute to the interplay with the conduction π carriers.

Finally we should comment on the feature which has a broad signal that predominates the observed ESR behavior. In agreement with the NEXAFS results, a stronger, sharp ESR signal of the edge state should have been observed for NR and NR1000, which have a larger amount of edge state. This apparent inconsistency between NEXAFS and ESR can be resolved if we consider the broad background signal in the ESR spectra observed in the NR, NR1000, and NR1500 samples. This background signal is naturally assigned to iron-including magnetic impurities, such as Fe or Fe_3O_4 nanoparticles produced in the CVD process with ferrocene as a precursor. On annealing at temperatures close to the melting points of Fe (1538 °C) and of iron oxide (Fe_3O_4) (1597 °C), the Fe and iron-oxide nanoparticles start to coagulate, and these magnetic nanoparticles have completely disappeared by 2000 °C, at which the Fe vapor pressure reaches several Torr. This is consistent with the ESR results in which the broad signal decreases in its intensity at 1500 °C and it completely disappears at 2000 °C.[34] Therefore, the absence of a narrow ESR peak in NR and NR1000 can be understood on the basis of the dipolar broadening of the ESR signal of edge-state spins from the magnetic impurities. The ferromagnetic iron-including nanoparticles present in the vicinity of the open edges give an inhomogeneously distributed strong ferromagnetic internal field to the edge-state spins, thereby broadening the ESR signal of the edge-state spins. This argument is further supported by the loop-formation phenomenon, which takes place by the reactivity of the bare edges at high temperatures.[31] As the annealing temperature reaches the melting point of the nanoparticles in NR1500, the magnetic nanoparticles start coagulating and become independent from the edge-state spins, as evidenced by the change in the feature of the ESR spectrum, in which the sharp edge-state spin signal and the broad magnetic nanoparticle signal coexist independently (see Fig. 4).

IV. SUMMARY

We investigated the edge state in graphene nanoribbons prepared by the CVD method, using carbon *K*-edge NEXAFS spectra and ESR spectra. The C 1*s* to π^* transition of graphene nanoribbon samples, which is free from the substrate-induced gap state and σ dangling bonds show a low-energy peak corresponding to the C 1*s* to edge-state transition of nanographene. The systematic decrease in the contribution of the edge state with increasing annealing temperature is well correlated with the decreasing population of nanographene edges due to loop formation in the presence of iron-including nanoparticles. The ESR signal assigned to the edge-state spin tracks the behavior of the NEXAFS spectra with fidelity. The temperature dependence of the ESR linewidth indicates that the edge-state spins are strongly coupled with the conduction *p* carriers. These experimental findings confirm the presence of a magnetic edge state in the edge of graphene nanoribbons and provide important additional findings about these magnetic edge states.

ACKNOWLEDGMENTS

The present work has been performed under the approval of Photon Factory Program Advisory Committee (PF-PAC, No. 2009G022). The authors are also grateful for the financial support of the Grant-in-Aid for Scientific Research, Grant No. 20001006 from the Ministry of Education, Culture, Sports, Science and Technology of Japan. We thank Y. Ishibashi and T. Takahashi for the assistance during the NEXAFS experiments.

[1] K. S. Novoselov, A. K. Geim, S. V. Morozov, D. Jiang, Y. Zhang, S. V. Dubonos, I. V. Grigorieva, and A. A. Firsov, Science **306**, 666 (2004).
[2] Y. Zhang, Y. Tan, H. L. Stormer, and P. Kim, Nature (London) **438**, 201 (2005).
[3] A. H. Castro Neto, F. Guinea, N. M. R. Peres, K. S. Novoselov and A. K. Geim, Rev. Mod. Phys. **81**, 109 (2009).
[4] M. Fujita, K. Wakabayashi, K. Nakada, and K. Kusakabe, J. Phys. Soc. Jpn. **65**, 1920 (1996).
[5] K. Nakada, M. Fujita, G. Dresselhaus, and M. S. Dresselhaus, Phys. Rev. B **54**, 17954 (1996).
[6] Y. Kobayashi, K. I. Fukui, T. Enoki, K. Kusakabe, and Y. Kaburagi, Phys. Rev. B **71**, 193406 (2005).
[7] Y. Kobayashi, K. I. Fukui, T. Enoki, and K. Kusakabe, Phys. Rev. B **73**, 125415 (2006).
[8] Y. Niimi, T. Matsui, H. Kambara, K. Tagami, M. Tsukada, and H. Fukuyama, Phys. Rev. B **73**, 085421 (2006).
[9] Z. Klusek, Z. Waqar, E. A. Denisov, T. N. Kompaniets, I. V. Makarenko, A. N. Titkov, and A. S. Bhatti, Appl. Surf. Sci. **161**, 508 (2000).
[10] T. Enoki, Y. Kobayashi, and K. Fukui, Int. Rev. Phys. Chem. **26**, 609 (2007).
[11] T. Enoki and K. Takai, Dalton Trans. **2008**, 3773.
[12] T. Enoki and K. Takai, Solid State Commun. **149**, 1144 (2009).
[13] K. Wakabayashi, M. Sigrist, and M. Fujita, J. Phys. Soc. Jpn. **67**, 2089 (1998).
[14] S. Entani, S. Ikeda, M. Kiguchi, K. Saiki, G. Yoshikawa, I. Nakai, H. Kondoh, and T. Ohta, Appl. Phys. Lett. **88**, 153126 (2006).
[15] M. Kiguchi, R. Arita, G. Yoshikawa, Y. Tanida, M. Katayama, K. Saiki, A. Koma, and H. Aoki, Phys. Rev. Lett. **90**, 196803 (2003).
[16] Y. Shibayama, H. Sato, T. Enoki, and M. Endo, Phys. Rev. Lett. **84**, 1744 (2000).
[17] Y. Shibayama, H. Sato, T. Enoki, X. Xin Bi, M. S. Dresselhaus, and M. Endo, J. Phys. Soc. Jpn. **69**, 754 (2000).
[18] V. L. Joseph Joly, K. Takai, and T. Enoki, J. Phys. Chem. Solids **71**, 575 (2010).
[19] V. L. Joseph Joly, K. Takahara, K. Takai, K. Sugihara, T. Enoki, M. Koshino, and H. Tanaka, Phys. Rev. B **81**, 115408 (2010).
[20] J. Campos-Delgado, J. M. Romo-Herrera, X. Jia, D. A. Cullen, H. Muramatsu, Y. A. Kim, T. Hayashi, Z. Ren, D. J. Smith, Y. Okuno, T. Ohba, H. Kanoh, K. Kaneko, M. Endo, H. Terrones, M. S. Dresselhaus, and M. Terrones, Nano Lett. **8**, 2773 (2008).

[21] J. Campos-Delgado, Y. A. Kim, T. Hayashi, A. Morelos-Gómez, M. Hofmann, H. Muramatsu, M. Endo, H. Terrones, R. D. Shull, M. S. Dresselhaus, and M. Terrones, Chem. Phys. Lett. **469**, 177 (2009).
[22] K. Amemiya, H. Kondoh, T. Yokoyama, and T. Ohta, J. Electron Spectrosc. Relat. Phenom. **124**, 151 (2002).
[23] H.-K. Jeong, H.-J. Noh, J.-Y. Kim, L. Colakerol, P.-A. Glans, M. H. Jin, K. E. Smith, and Y. H. Lee, Phys. Rev. Lett. **102**, 099701 (2009).
[24] H.-K. Jeong, L. Colakerol, M. H. Jin, P.-A. Glans, K. E. Smith, and Y. H. Lee, Chem. Phys. Lett. **460**, 499 (2008).
[25] J. C. Lascovich, R. Giorgi, and S. Scaglione, Appl. Surf. Sci. **47**, 17 (1991).
[26] M. Maruyama and K. Kusakabe, J. Phys. Soc. Jpn. **73**, 656 (2004).
[27] G. U. Sumanasekera, G. Chen, K. Takai, J. Joly, N. Kobayashi, T. Enoki, and P. C. Eklund, J. Phys.: Condens. Matter (to be published).
[28] D. Pacilé, M. Papagno, A. Fraile Rodríguez, M. Grioni, L. Papagno, Ç. Ö. Girit, J. C. Meyer, G. E. Begtrup, and A. Zettl, Phys. Rev. Lett. **101**, 066806 (2008).
[29] T. Koyama and M. Endo, Jpn. J. Appl. Phys. **13**, 1175 (1974).
[30] Z. Liu, K. Suenaga, P. J. F. Harris, and S. Iijima, Phys. Rev. Lett. **102**, 015501 (2009).
[31] E. Cruz-Silva, A. R. Botello-Mëndez, Z. Barnett, X. Jia, M. S. Dresselhaus, H. Terrones, M. Terrones, B. G. Sumpter, and V. Meunier (private communication).
[32] H. Hasegawa, Prog. Theor. Phys. **21**, 483 (1959).
[33] R. H. Taylor, Adv. Phys. **24**, 681 (1975).
[34] In agreement with the ESR broad signal, ferromagnetic impurities were detected in the magnetization of the pristine sample at room temperature. The spontaneous magnetization associated with the iron impurities decreased with increasing annealing temperature, and eventually disappeared in NR2000.